BIOCELL
2024 48(4): 665-675

Tech Science Press

Inhibition of SLC26A4 regulated by electroacupuncture suppresses the progression of myocardial ischemia-reperfusion injury

Fei KONG[1]; Qiyuan TIAN[2]; Binglin KUANG[3]; Lili SHANG[4]; Xiaoxiao ZHANG[5]; Dongyang LI[5]; Ying KONG[6,*]

[1] Department of Endocrinology, Heilongjiang University of Chinese Medicine, Harbin, 150040, China
[2] Department of Cardiology, Heilongjiang University of Chinese Medicine, Harbin, 150040, China
[3] College of Clinical Medicine, Heilongjiang University of Chinese Medicine, Harbin, 150040, China
[4] Department of Nephrology, Beijing Hospital of Integrated Traditional Chinese and Western Medicine, Beijing, 100039, China
[5] College of Acupuncture and Massage, Heilongjiang University of Chinese Medicine, Harbin, 150040, China
[6] Department of Acupuncture, Heilongjiang University of Chinese Medicine, Harbin, 150040, China

Key words: Myocardial ischemia, Reperfusion, SLC26A4, NF-κB pathway

Abstract: Introduction: Myocardial ischemia-reperfusion (IR) injury has received widespread attention due to its damaging effects. Electroacupuncture (EA) pretreatment has preventive effects on myocardial IR injury. SLC26A4 is a Na+ independent anion reverse transporter and has not been reported in myocardial IR injury. **Objectives:** To find potential genes that may be regulated by EA and explore the role of this gene in myocardial IR injury. **Methods:** RNA sequencing and bioinformatics analysis were performed to obtain the differentially expressed genes in the myocardial tissue of IR rats with EA pretreatment. Myocardial infarction size was detected by TTC staining. Serum CK, creatinine kinase-myocardial band, Cardiac troponin I, and lactate dehydrogenase levels were determined by ELISA. The effect of SLC26A4 on cardiomyocyte apoptosis was explored by TUNEL staining and western blotting. The effects of SLC26A4 on inflammation were determined by HE staining, ELISA, and real-time PCR. The effect of SLC26A4 on the NF-κB pathway was determined by western blotting. **Results:** SLC26A4 was up-regulated in IR rats but downregulated in IR rats with EA pretreatment. Compared with IR rats, those with SLC26A4 knockdown exhibited improved cardiac function according to decreased myocardial infarction size, reduced serum LDH/CK/CK-MB/cTnI levels, and elevated left ventricular ejection fraction and fractional shortening. SLC26A4 silencing inhibited myocardial inflammation, cell apoptosis, phosphorylation, and nuclear translocation of NF-κB p65. **Conclusion:** SLC26A4 exhibited promoting effects on myocardial IR injury, while the SLC26A4 knockdown had an inhibitory effect on the NF-κB pathway. These results further unveil the role of SLC26A4 in IR injury.

Introduction

Acute myocardial infarction (AMI) is a form of cardiovascular disease with high mortality and morbidity worldwide, which is caused by acute or persistent hypoxia and ischemia in the coronary arteries. AMI is usually characterized by left ventricular dilation, heart failure, and sudden cardiac death [1,2]. Thrombolytic drugs and surgical treatments effectively restore cardiac perfusion after AMI [3]. A reperfusion of the heart following ischemia can result in a significant resumption of function. However, the reperfusion may induce myocardial ischemia-reperfusion [IR] injury [4], to cause inflammation, cell death, and various pathologies, and reduce the benefits of perfusion therapy [5]. A large number of studies shown that inhibiting the inflammatory response during IR is an important means to effectively relieve the damage [6,7]. Therefore, reducing the inflammatory damage caused by IR and improving the postoperative survival rate of AMI patients has become an urgent problem to be solved when treating AMI.

Solute carrier family 26 member 4 (SLC26A4, or pendrin) is a Na^+ independent anion reverse transporter and plays an important role in many diseases such as cancer, hearing damage, airway inflammation, hypertension, and cardiac hypertrophy [8–12]. In a previous study, SLC26A4 was upregulated in congestive heart failure samples [13]. SLC26A4 can regulate the expression of

*Address correspondence to: Ying Kong, feifei04588878@163.com
Received: 27 September 2023; Accepted: 05 December 2023;
Published: 09 April 2024

Doi: 10.32604/biocell.2024.046342

inflammatory cytokines; SLC26A4 knockdown reduced the levels of tumor necrosis factor-α (TNF-α), interferon-γ, and interleukin-17 (IL-17) and decreased the inflammasome activity and prevented airway inflammation [10]. Inhibition of SLC26A4 also reduced allergic airway inflammation by increasing regulatory T cells and reducing levels of inflammatory cytokines IL-4, IL-5, and IL-13 [14]. In addition, SLC26A4 inhibition reduced the levels of Tumour Necrosis Factor alpha, IL-1β, and IL-6 and blocked the NF-κB pathway, thereby reducing lipopolysaccharide-induced acute injury [15]. At present, the effect of SLC26A4 on the inflammation caused by IR remains unclear.

Electroacupuncture (EA), a modified acupuncture treatment method, has been widely used in inflammatory disease [16]. Clinically, EA pretreatment can prevent myocardial injury. For example, EA treatment before heart valve replacement surgery reduced postoperative myocardial ischemia-reperfusion injury in patients [17]. EA treatment before percutaneous coronary intervention (PCI) surgery decreased the cardiac troponin I (cTnI) level and protected patients with coronary heart disease from myocardial injury after PCI [18]. EA pretreatment at Neiguan (PC6) protected rat myocardium from IR injury [19,20]. All above reports demonstrate the cardioprotective effects of EA pretreatment. The mechanism by which EA pretreatment exerts a pre-protective effect on the myocardium is not completely clear. Our sequencing data showed a significantly increased level of SLC26A4 in the myocardial tissue of IR rats, but a decreased level in IR rats with EA pretreatment. Based on the existing research reports of SLC26A4 and our sequencing results, the role of SLC26A4 in IR attracted our attention.

Nuclear factor kappa light chain enhancer of activated B cells (NF-κB) is closely associated with inflammation. NF-κB activation regulates the expression of inflammatory cytokines [21]. NF-κB, a critical regulator of inflammatory responses, has long been considered a prototypical proinflammatory nuclear factor and the holy grail as an anti-inflammatory target [22]. Furthermore, NF-κB is a major transcription factor associated with cardiovascular disease [23]. Previous studies have shown that inhibition of NF-κB plays a protective role in myocardial IR injury [24]. EA at PC6 reduced the expression of inflammatory cytokines in serum or myocardial tissue [25]. In the research of other diseases, the possible molecular mechanism by which EA regulates inflammation has been explored [26]. Importantly, EA at PC6 has been shown to regulate the NF-κB pathway [27,28]. SLC26A4 is positively related to the levels of inflammatory cytokines, according to previous studies. It is not known whether SLC26A4, a possible target gene of EA, mediates inflammatory response through NF-κB in myocardial IR tissues.

Based on the above research background, we speculated that SLC26A4 might play an important role in the IR process and have an important connection to the NF-κB signaling pathway.

Materials and Methods

Experimental animals

All animal experiments were performed under the approval of the Ethics Committee of the Fourth Affiliated Hospital of Heilongjiang University of Chinese Medicine (No. 19 in 2022). We randomly divided 18 healthy male Sprague-Dawley (SD) rats into three groups, which were named sham, IR, and IR+EA. The rats were fed freely with water and foods at 22°C ± 1°C in a cycle of 12 h light and 12 h dark. Anesthesia was induced by 5% isoflurane and maintained by 1%–2% isoflurane in 100% O_2. EA pretreatment was performed at PC6 acupoint (1.5 cm proximal to the crease of the palm just above the median nerve) on both forelimbs of rats using a low-frequency pulse therapeutic apparatus (G6805-I, Qingdao Xinsheng Industrial Co., Ltd., Shandong, China) for 12 days (20 min each day). EA stimulation at PC6 acupoints has been shown to reduce myocardial ischemia in many studies [29–31]. The acupuncture needles were inserted into the subcutaneous tissue at a depth of 2–3 mm and secured with plastic tape. The frequency of EA pretreatment was set to 2/15 Hz (dense-scattered alternating mode) [30,32], and the current intensity was set to 1 mA. IR injury was induced by left anterior descending (LAD) coronary artery occlusion within 30 min post the EA pretreatment. After occlusion for 30 min, the reperfusion was conducted for 4 h [33,34]. Rats in the sham group received the same operation without the coronary artery occlusion. Rats were sacrificed by an overdose of CO_2. The RNA was extracted from the myocardial tissues of rats for mRNA sequencing. Blood samples were collected for follow-up experiments.

Ninety-six healthy male SD rats were included, and divided into four groups: the sham, IR, IR+siNC, and IR +siSlc26a4 groups. Rats were intramyocardially injected with 20 μg of SLC26A4 siRNA (siSlc26a4) or negative control siRNA (siNC), followed by LAD coronary artery occlusion after 48 h. The sense sequences of siRNA used in this section were as follows: siSlc26a4: 5′-GCUGCAGUUGCU CAAGAAATT-3′; siNC: 5′-UUCUCCGAACGUGUCACGU TT-3′. LAD coronary artery occlusion was performed with the same operation as mentioned above. Collection of blood and left ventricular myocardium from rats was conducted for the following experiments.

RNA sequencing

The myocardial tissue samples were sent to Hangzhou Lianchuan Bio Technologies Co. (Zhejiang, China) for transcriptional sequencing. Total RNA was isolated and purified using TRIzol reagent (Invitrogen, CA, USA). NanoDrop ND-1000 (NanoDrop, DE, USA) was used to quantify the RNA concentration. Sequencing data were aligned to rat genomes through HISAT2 (https://ccb.jhu.edu/software/hisat2). We used the StringTie software (http://ccb.jhu.edu/software/stringtie/) to assemble the transcripts and the FPKM method to quantify them. The differential genes among the samples were analyzed using the edgeR package (https://bioconductor.org/packages/release/bioc/html/edgeR.html). Finally, Gene Ontology (GO) and Kyoto Encyclopedia of Genes and Genomes (KEGG) enrichment analysis were performed using DAVID software (https://david.ncifcrf.gov/).

Echocardiography

The anesthetized rats were fixed on a table with their limbs and subjected to depilation of the chest hair. Observation

and recording of echocardiogram were conducted using the vevo2100 ultra-high resolution small animal ultrasound imaging system (FUJIFILM VisualSonics, Toronto, Canada).

Hematoxylin-eosin (HE) staining

After dehydration, the fixed left ventricular myocardium was embedded in paraffin and then sliced. Paraffin sections were dewaxed twice with xylene for 15 min each and soaked in ethanol with different concentrations (100%, 95%, 85%, and 75%), then soaked in distilled water for 2 min. The slides were stained with hematoxylin (Solarbio, Beijing, China) and eosin (Sangon, Shanghai, China) (HE). The stained sections were dehydrated with absolute ethanol, transparentized with xylene, and sealed with neutral gum. A BX53 (Olympus, Tokyo, Japan) microscope was used to observe the staining.

2,3,5-Triphenyltetrazolium chloride (TTC) staining

The hearts were removed from sacrificed SD rats, rinsed with normal saline, and then frozen at −20°C for 3 h. Next, heart tissue was cut into five pieces, and stained with 2 mL 2% TTC-staining solution (2,3,5-triphenyltetrazolium chloride [TTC] was dissolved in 0.01 M phosphate buffered saline [PBS]) at 37°C for 15 min in the dark condition. Another staining was conducted for 15 min after the heart slices were turned over. The staining results were recorded and the size was calculated using the Image Pro Plus 6.0 (Media Cybernetics, MD, USA).

Real-time polymerase chain reaction (qPCR)

TRIpure (Bioteke, Beijing, China) lysate, chloroform, and isopropanol were used to extract total RNA from left ventricular myocardium. The RNA concentration was detected by a NANO 2000 spectrophotometer (ThermoFisher Scientific, PA, USA). Next, cDNA was obtained by reverse transcription of RNA using BeyoRT II M-MLV reverse transcriptase (Beyotime, Shanghai, China). The reaction mix comprised: cDNA (1 μL), 2 × Taq PCR MasterMix (10 μL) (Solarbio, Beijing, China), SYBR Green (0.3 μL) (Solarbio, Beijing, China), and 10 μM primer (0.5 μL of each primer), mixed and the amplification was detected by ExicyclerTM 96 fluorescence quantitation instrument. The primer sequences were as follows, rat SLC26A4 F: 5′-GTTCAGTTCCCTTCGTGG-3′; rat SLC26A4 R: 5′-TGCTTTCAGCCTCTTGTT-3′; rat TNF-α F: 5′-CGGAAAGCATGATCCGAGAT-3′; rat TNF-α R: 5′-AGACAGAAGAGCGTGGTGGC-3′; rat IL-1β F: 5′-TTCAAATCTCACAGCAGCAT-3′; rat IL-1β R: 5′-CACGGGCAAGACATAGGTAG-3′; rat IL-6 F: 5′-CAGCCACTGCCTTCCCTA-3′; rat IL-6 R: 5′-TTGCCATTGCACAACTCTTT-3′. The $2^{-\Delta\Delta CT}$ method was applied to analyze the PCR data.

Western blotting (WB)

Total protein was extracted from the left ventricular myocardium of rats using a cell lysis buffer for western blotting and immunoprecipitation (Beyotime, Shanghai, China), and the nuclear protein of myocardial tissue was extracted using a Nuclear and Cytoplasmic Protein Extraction Kit (Beyotime, Shanghai, China). The BCA protein assay kit (Beyotime, Shanghai, China) was used to determine the protein concentration. Then, 20 μL of protein with nearly the same concentration was separated by sodium dodecylsulfate-polacrylamide gel electrophoresis (SDS-PAGE), and transferred to polyvinylidene fluoride membranes (Millipore, MA, USA), which was blocked with skim milk (5%). The membranes were incubated overnight with the specific primary antibody at 4°C, and followed by incubation with the secondary antibody at 37°C for 45 min. The antibodies were as follows: SLC26A4 (A16413, ABclonal, Beijing, China), NF-κB p65 (A2547, ABclonal), p-NF-κB p65 (AF2006, Affinity, OH, USA), cleaved Caspase-3 (AF7022, Affinity,), cleaved caspase-9 (10380-1-AP, Proteintech, IL, USA), Bax (A19684, ABclonal), Bcl-2 (A0208, ABclonal), goat anti-rabbit IgG (A0208, Beyotime, Shanghai, China), goat anti-mouse IgG (A0216, Beyotime), histone H3 (AM8433, Abgent, CA, USA), and β-actin (sc-47778, Santa Cruz, CA, USA). Finally, the target protein was detected by enhanced chemiluminescence (ECL). Due to the small difference in the molecular weight of several proteins (Bax: 21 kDa; Bcl-2: 26 kDa; cleaved Caspase-3: 17 kDa and cleaved Caspase-3: 35 kDa), their SDS-PAGE were conducted in two batches, and each experiment had an internal control (β-actin).

Enzyme-linked immunosorbent assay (ELISA)

The rat myocardial tissue was homogenized mechanically in normal saline on ice, and the supernatant after homogenization was detected by a BCA protein concentration assay kit (Solarbio, Beijing, China). Standard products of rat TNF-α, IL-1β, cTnI, and IL-6 were prepared according to specific instructions of the ELISA kits for rat TNF-α, rat IL-6, rat cTnI, and rat IL-1β. Rat cTnI ELISA kit was purchased from Wuhan Fine Biotech Co., Ltd. (Wuhan, China), and the others were purchased from Multisciences (Zhejiang, China). The OD value of each sample at 450 and 570 nm was detected by a microplate reader (ELX-800, BIOTEK, VT, USA).

Assay kits for creatine kinase (CK), creatine kinase MB (CK-MB) isoenzyme, and lactate dehydrogenase (LDH) were used to detect the activities of CK, CK-MB, and LDH in rat serum, respectively, according to the instructions. The three kits were purchased from Nanjing Jiancheng Bioengineering Institute (Nanjing, China).

Terminal deoxynucleotidyl transferase dUTP nick end labeling (TUNEL) assay

Triton X-100 (Beyotime, Shanghai, China) (50 μL 0.1% Triton X-100 dissolved in 50 mL of 0.1% lemon salt) was applied to slides for 8 min. Sections were washed thrice with PBS for 5 min per wash, followed by TUNEL detection in accordance with In Situ Cell Death Detection Kit (Roche, Switzerland). Sections were counterstained with 4′,6-diamidino-2-phenylindole (DAPI; Aladdin, Shanghai, China) in the dark for 5 min. After washing thrice with PBS, the sections were sealed with a fluorescence quencher and observed under a BX53 microscope.

Statistical analysis

All data were analyzed using GraphPad Prism 8 software with the one-way ANOVA method. All data are presented as mean ± SD, and $p < 0.05$ indicates a significant difference.

Results

Bioinformatics analysis of RNA sequencing data from ischemia-reperfusion rats with electroacupuncture pretreatment

On the premise that EA pretreatment is known to have a preventive effect on myocardial IR injury, to explore the underlying mechanism, we first searched the PubMed database using the keyword "Electroacupuncture pretreatment," and 101 results appeared. These articles included 2 reviews and 99 experimental articles. Among these experimental articles, 29 were related to inflammation and 40 to apoptosis (Fig. 1A). The above data led us to preliminarily conclude that the key directions of this study were inflammation and apoptosis. Second, the animal model of IR was established, and mRNA sequencing was performed to find the potential target of EA pretreatment. Myocardial IR injury was induced by LAD coronary artery occlusion in SD rats with EA pretreatment. Serum levels of LDH and CK in SD rats were determined by kits, and it showed that the serum levels of LDH and CK were increased in the IR group, but EA pretreatment decreased their serum levels (Figs. 1B and 1C). RNA sequencing of myocardial tissues was performed to analyze the differentially expressed genes (DEGs) between the three groups. Principal component analysis of RNA sequencing data from these groups showed the clear separation of the samples (Fig. 1D). Bioinformatics analysis of RNA sequencing data yielded 1,094 up-regulated genes and 159 downregulated genes in the IR group compared with the sham group, according to $|\log2FoldChange| > 1$ and p-value < 0.05. The comparison between the IR+EA group and the IR group yielded 309 up-regulated genes and 76 downregulated genes. The SLC26A4 gene was up-regulated in the myocardial tissue of IR rats and downregulated in the myocardial tissue of IR rats with EA pretreatment (Fig. 1E). In addition, we searched the GeneCards website using the keyword "myocardial injury" to obtain genes related to myocardial injury. Venn diagram showed the number of overlapping genes between the up-regulated genes in IR/sham groups and the down-regulated genes in IR+EA/IR groups, and genes from the GeneCards website (Fig. 1F). Twelve overlapping genes were obtained and their log2FoldChange (Log2FC) and p-value are presented in the scatterplot in Fig. 1F. We sorted these genes based on their Log2FC values and gathered information about each gene. Among the seven genes compared to SLC26A4, six genes (*Pnoc*, *Phex*, *Krt14*, *Nefh*, *Krt7*, and *Cfi*) do not have published reports of their involvement in heart-related diseases, while one (*Lrp2*) has been reported in heart-related studies; however, these studies have revealed that Lrp2 is closely related to congenital heart disease and heart development. Only SLC26A4 has been reported in several cardiac studies to be associated with cardiac hypertrophy and heart failure [12,13,35]. Furthermore, SLC26A4 has been found to inhibit inflammation [14,15]. These reports aroused our interest in SLC26A4, although, to the best of our knowledge, there are no reports of SLC26A4 in myocardial IR injury. Therefore, we decided to explore the role of SLC26A4 in myocardial IR injury. GO and KEGG enrichment analysis on all DEGs revealed that inflammation and apoptosis-related functional annotations and pathway terms were more abundant. Figs. 1G and 1H present several representative annotations and terms.

Silencing of SLC26A4 improved cardiac function in Sprague-Dawley rats

Rats were intramyocardially injected with 20 μg SLC26A4 siRNA to knock down SLC26A4. After 48 h, myocardial IR injury was induced by LAD coronary artery occlusion in the rats for 30 min. Then reperfusion was performed for 4 h (Fig. 2A). The protein and mRNA levels of SLC26A4 determined by western blotting and qPCR, respectively, revealed inhibition of SLC26A4 in the IR+siSlc26a4 group (Figs. 2B and 2C). The original image of the immunoblot is mentioned in Supplementary Materials. TTC staining to determine the size of the myocardial infarct showed that the knockdown of SLC26A4 inhibited myocardial infarction (Fig. 2D). Silencing of SLC26A4 decreased the serum levels of LDH, CK, CK-MB, and cTnI in SD rats with IR injury (Figs. 2E–2H). Left ventricular end-diastolic dimension (LVEDD), left ventricular end-systolic dimension (LVESD), and left ventricular ejection fraction (LVEF) assessed by echocardiography are important indexes of cardiac function. The percentage of left ventricle fractional shortening (LVFS) was calculated using the equation LVFS = (LVEDD – LVESD)/LVEDD × 100%. Fig. 2I shows the representative echocardiogram and the analysis of cardiac function indexes. LVEDD and LVESD increased in the IR+siNC group but decreased in the SLC26A4 knockdown group. Compared with IR+siNC group, LVFS (%) and LVEF (%) increased in the SLC26A4 knockdown group. Therefore, SLC26A4 knockdown alleviated myocardial IR injury.

Knockdown of SLC26A4 inhibited the cell apoptosis of myocardial tissue from ischemia-reperfusion rats

Myocardial tissue with SLC26A4 silencing stained with TUNEL reagent showed that silencing of SLC26A4 reduced the number of apoptotic cells (Fig. 3A). To further evaluate the effect of SLC26A4 on cardiomyocyte apoptosis, the protein levels of Bax, Bcl-2, cleaved caspase-3, and cleaved caspase-9 were detected by western blotting. In the group of SLC26A4 knockdown, the protein levels of Bax, cleaved caspase-3, and cleaved caspase-9 were decreased compared with those of the IR group, but the level of Bcl-2 protein increased (Fig. 3B).

Silencing of SLC26A4 suppressed myocardial inflammation and nuclear factor-kappa B pathway in Sprague-Dawley rats

HE staining of myocardial tissue revealed remarkable myofibrillar loss, cytoplasmic vacuolization, and inflammatory cell infiltration in IR group and IR+siNC group, while these symptoms were relieved in IR+siSlc26a4 group (Fig. 4A). The analysis of relative mRNA and protein levels of inflammatory cytokines including TNF-α, IL-6, and IL-1β showed that inhibition of SLC26A4 suppressed their expression (Figs. 4B and 4C). To determine whether

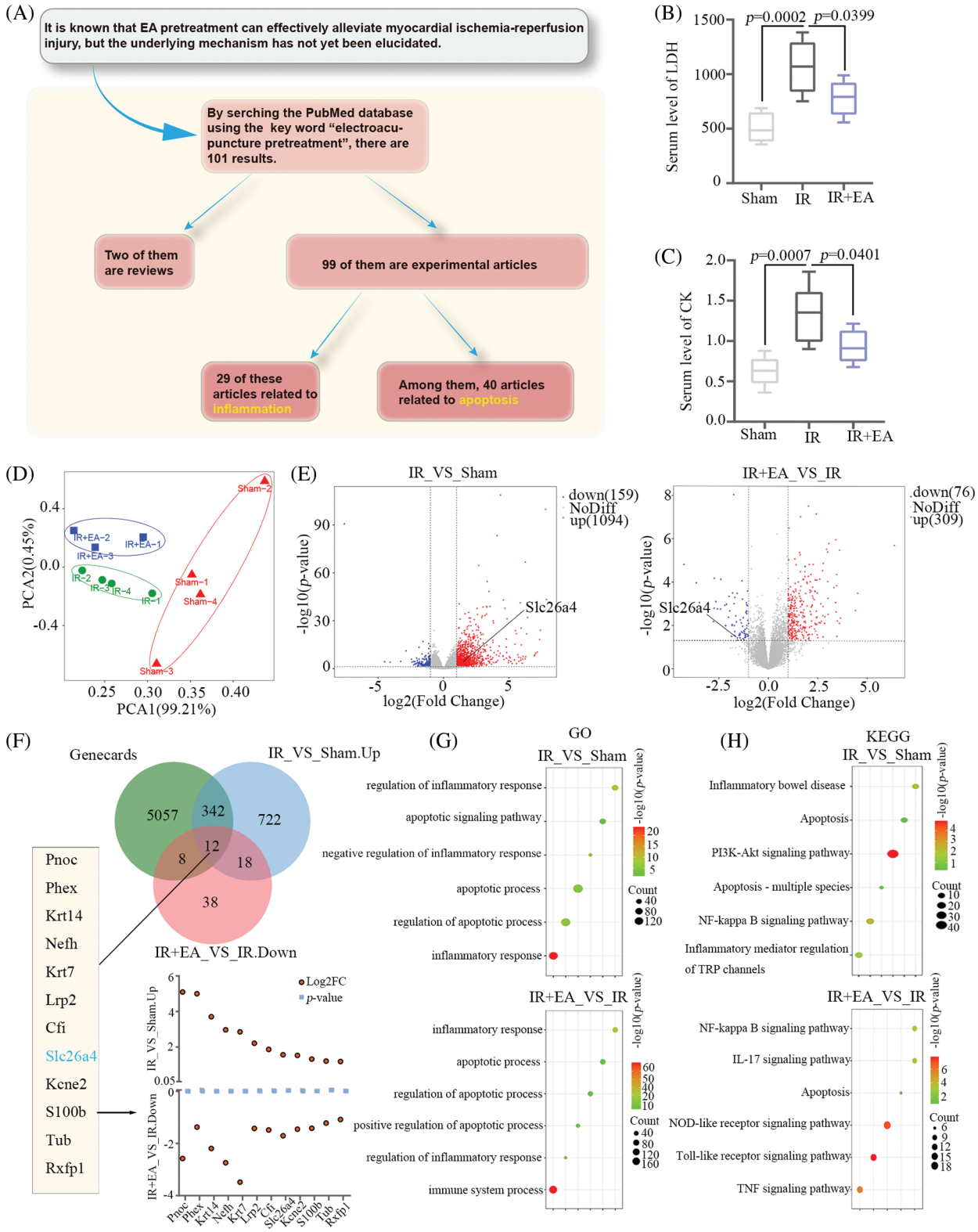

FIGURE 1. Bioinformatics analysis of RNA sequencing data from ischemia-reperfusion (IR) rats with electroacupuncture (EA) pretreatment. (A) Workflow of research direction identified through PubMed website. (B) Serum level of lactate dehydrogenase (LDH) in rats of the three groups (sham, IR, and IR+EA), n = 6 in each group. (C) Serum level of creatine kinase (CK) in rats, n = 6 in each group. All data are expressed as mean ± SD. The total RNA of the myocardial tissues from rats in the three groups was extracted and sequenced. (D) Principal component analysis (PCA) of rat mRNA between the three groups. (E) Volcano plot of 1253 DEGs (IR group *vs.* sham group) and 385 DEGs (IR+EA group *vs.* IR group). (F) Venn plot of genes from IR *vs.* sham group and IR+EA *vs.* IR group and GeneCards (https://www.genecards.org/). (G and H) Gene Ontology (GO) and Kyoto Encyclopedia of Genes and Genomes (KEGG) pathway enrichment analysis were conducted on these differentially expressed genes (log2FoldChange > 1 and p value < 0.05) of the three groups. Representative functional annotations were shown in G, and pathway terms were shown in H.

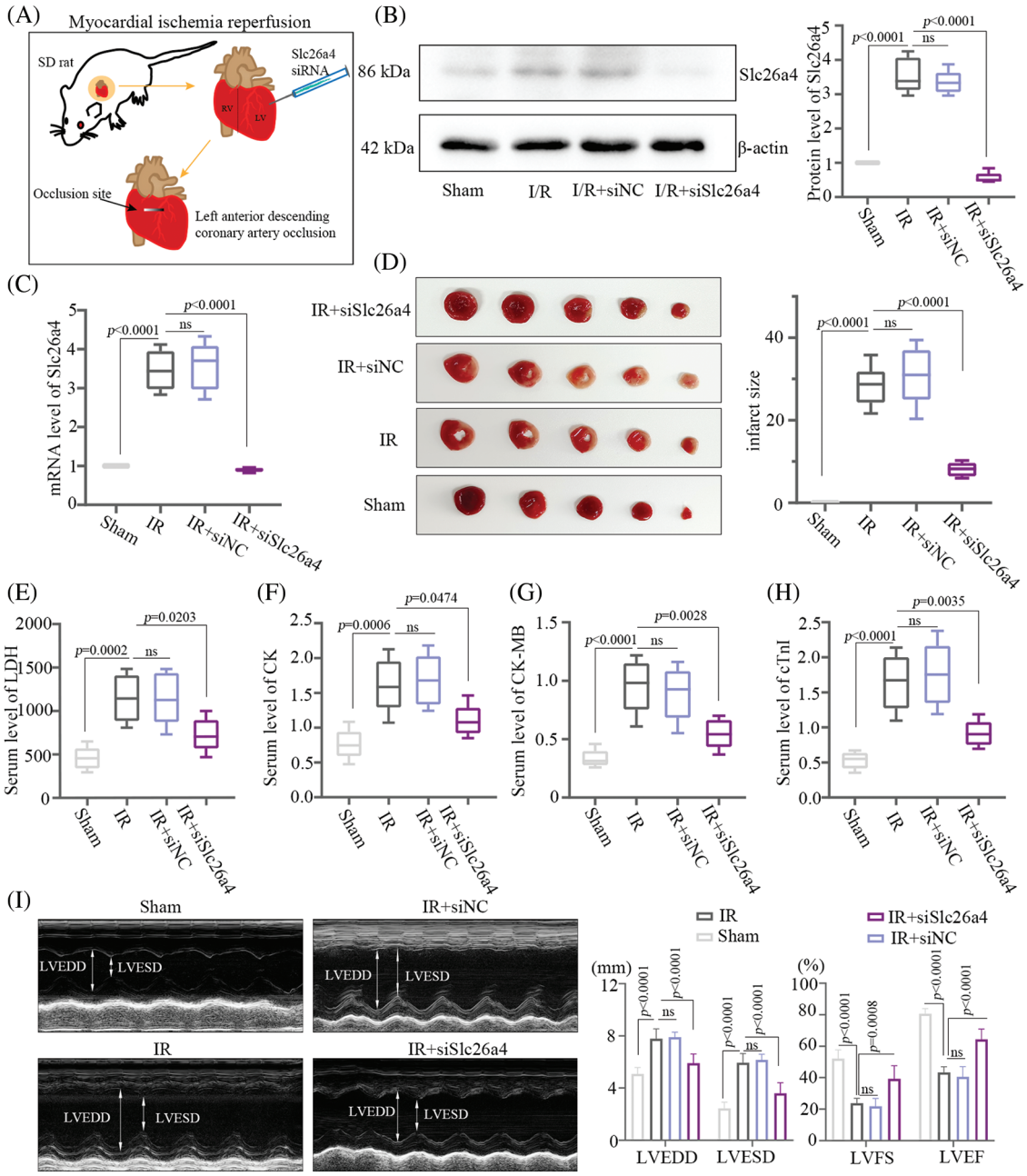

FIGURE 2. SLC26A4 silencing improved cardiac function in Sprague-Dawley (SD) rats. (A) Schematic diagram depicting the experimental protocols of myocardial ischemia-reperfusion (IR) injury in SD rats induced by left anterior descending (LAD) coronary artery occlusion with injection of SLC26A4 siRNA. Rats were intramyocardially injected with 20 μg of SLC26A4 siRNA to knock down SLC26A4. After 48 h, myocardial IR injury was induced by ligating the left anterior descending coronary artery in the rats. After 30 min of ischemia, reperfusion was performed for 4 h. (B) Detection of SLC26A4 protein by western blotting. (C) Determination of the mRNA level of SLC26A4. (D) Myocardial infarction was detected by 2,3,5-Triphenyltetrazolium chloride (TTC) staining. The analysis of myocardial infarct size is shown in the right panel. (E) Serum level of LDH. (F) Serum level of creatine kinase (CK). (G) Serum level of CK-MB. (H) Serum level of cardiac troponin I (cTnI). (I) Echocardiographic evaluation of effects of SLC26A4-knockdown on cardiac function, and quantitative analysis of left ventricular end-diastolic dimension (LVEDD), left ventricular end-systolic dimension (LVESD), left ventricle fractional shortening (LVFS) and left ventricular ejection fraction (LVEF) are shown in the right panel (n = 6 in each group). All data are expressed as mean ± SD.

SLC26A4 knockdown inhibits the myocardial inflammation through the NF-κB signaling pathway, we assessed the level of NF-κB p65 and phosphorylated NF-κB p65 (Ser536) proteins and found that inhibition of SLC26A4 decreased the level of phosphorylated NF-κB p65 (Fig. 5A). In addition, the protein level of NF-κB p65 in the nucleus was decreased in IR+siSlc26a4 group (Fig. 5B).

Discussion

A number of studies have reported the protective effects of EA at PC6 acupoint on myocardial IR injury; these effects include improvement in cardiac function and energy metabolism, promotion of post-ischemia angiogenesis [36], reduction in the release of cardiac troponin I [18], protection of

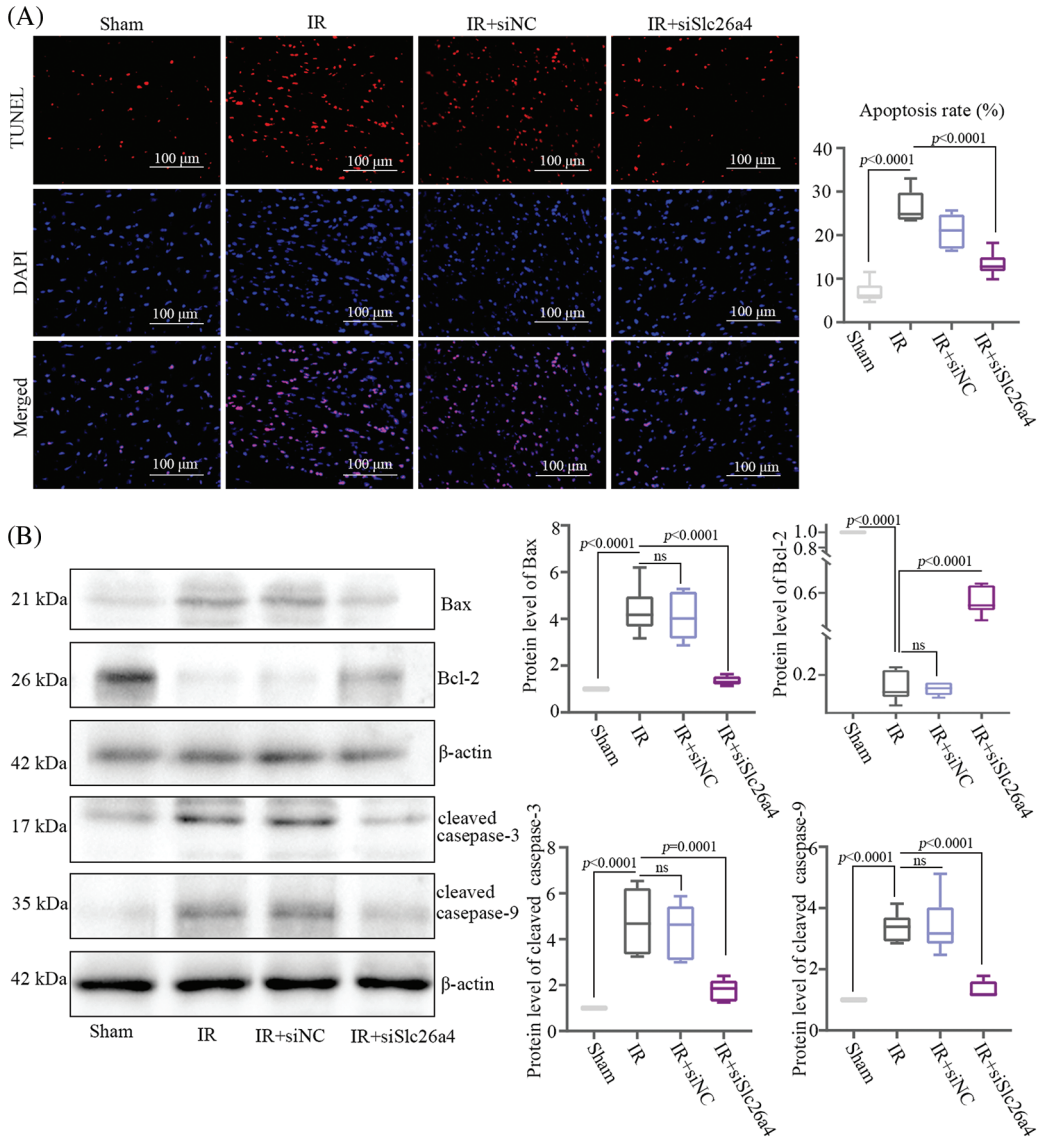

FIGURE 3. Knockdown of SLC26A4 inhibited myocardial tissue apoptosis. (A) Cell apoptosis of myocardial tissue in ischemic penumbra detected by terminal deoxynucleotidyl transferase dUTP nick end labeling (TUNEL) staining; bar = 100 μm. The right column indicates quantitative results of TUNEL-positive areas. (B) Determination of Bax, Bcl-2, cleaved caspase-3, cleaved caspase-9 protein levels by western blotting (n = 6 in each group). All data were expressed as mean ± SD.

myocardial muscle from damage, and antiarrhythmic effects [37]. However, the mechanism of the protective effect of EA preconditioning PC6 on myocardial IR has not yet been elucidated. This study reveals some overlaps between the up-regulated genes induced by EA pretreatment and the down-regulated genes induced by IR. Concurrently, multiple identical genes between EA-induced down-regulated genes and IR-induced up-regulated genes also exist. EA pretreatment might alleviate the myocardial IR injury by altering the gene expression of myocardial IR tissue. In this study, SLC26A4, up-regulated in the IR group and down-regulated in the IR+EA group, might be a potential target gene for EA pretreatment. Further investigation is needed to prove the possibility. This study shows that SLC26A4 knockdown could alleviate myocardial IR injury. However, we did not confirm the effect of SLC26A4 on IR rats with EA pretreatment. Another shortcoming of this study is that the role of SLC26A4 in IR was only verified *in vivo* but not *in vitro*. The molecular mechanism of the role of SLC26A4 in apoptosis and inflammation at the cellular level is of great interest, and we will consider this topic as a top priority for future research.

SLC26A4 has been extensively studied in hearing loss, thyroid cancer [38], and gastric cancer [39]. Several studies have reported that the function of SLC26A4 is related to the heart and blood pressure. In one study, hypertension was suppressed in rats with the SLC26A4 mutation in 2003 [11]. In 2016, the above research result was confirmed in humans, and the blood pressure of patients with SLC26A4 mutation was lower than that of the control group. They also found significantly reduced left ventricular hypertrophy index in patients with SLC26A4 mutation [35]. In 2019, Tang et al. reported that SLC26A4 is significantly up-regulated in PE-induced cardiac hypertrophy, and the inhibition of SLC26A4 reduced the expression of α-SMA, promoted the expression of glycogen synthase kinase-3 beta and apoptosis of cardiac mast cells, and alleviated cardiac hypertrophy [12]. Currently, there is

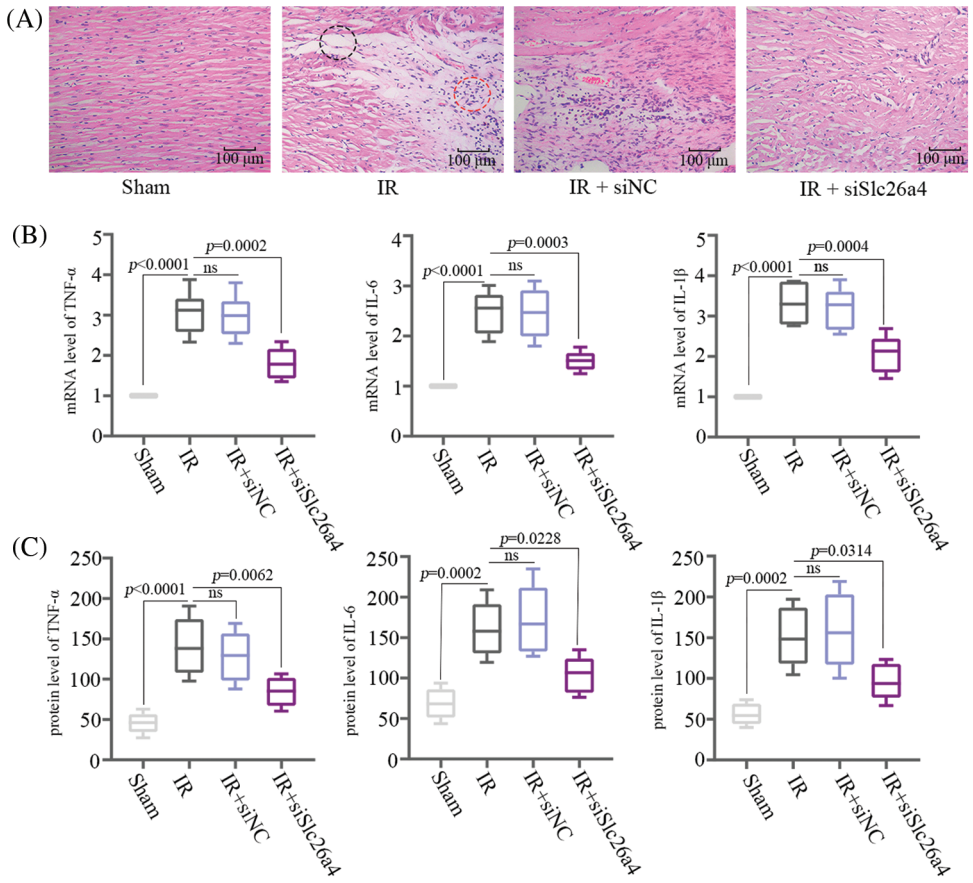

FIGURE 4. SLC26A4 silencing suppressed myocardial Inflammation in Sprague-Dawley rats. (A) Hematoxylin and eosin staining of histopathological changes in myocardial tissue. The black circle shows myofibrillar loss and cytoplasmic vacuolization, and the red circle indicates inflammatory cell infiltration; bar = 100 μm. (B) The mRNA levels of tumor necrosis factor-α (TNF-α), interleukin-6 (IL-6), and IL-1β. (C) The protein levels of TNF-α, IL-6, and IL-1β detected by enzyme-linked immunosorbent assay (n = 6 in each group). All data are expressed as mean ± SD.

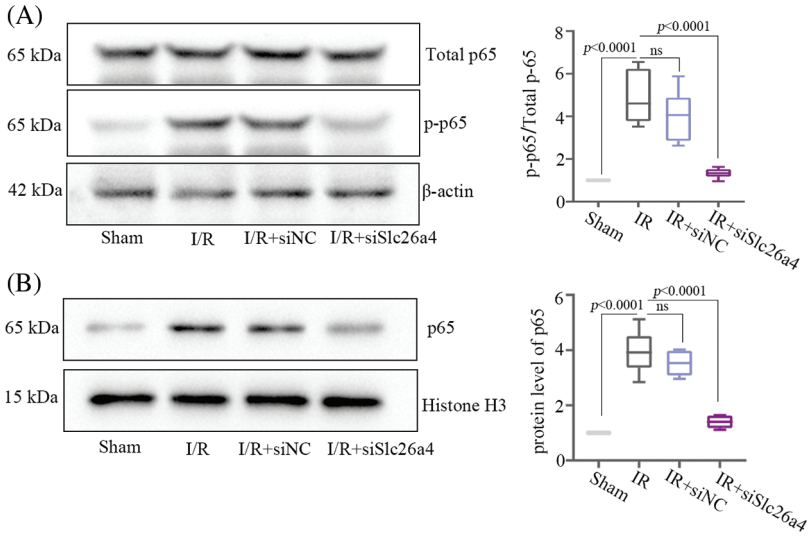

FIGURE 5. SLC26A4 silencing inhibited the nuclear factor-kappa B (NF-κB) pathway in rat cardiomyocytes. (A) Protein levels of NF-κB p65, and p-NF-κB p65 (Ser536) in the cytoplasm were detected by western blotting. (B) Protein levels of NF-κB p65 in the nucleus was detected by western blotting (n = 6 in each group). All data were expressed as mean ± SD.

no report on the role of SLC26A4 in IR and this study is the first to link SLC26A4 with myocardial IR injury. Our study found that SLC26A4 knockdown relieved myocardial IR injury and inhibited cardiomyocyte apoptosis and myocardial inflammation. All the above-mentioned results suggested a negative correlation of SLC26A4 with cardiac function.

NF-κB is a homologous or heterologous dimer composed of different subunits of the Rel family of proteins, including RelA (p65), RelB, c-Rel, p50 (NF-κB1), and p52 (NF-κB2)

[40]. Among these, the dimer of p65 and cRel is involved in the most classical NF-κB signaling pathway [41]. NF-κB plays an important role in regulating inflammation. Several studies have reported different molecules that target subunit p65 to mediate inflammation; these molecules affect p65 activation in different ways, including interaction with the IκB complex, prevention/promotion of p65 nuclear translocation, activation of nuclear p65, and post-translational modifications [42–45]. The reported mechanism of the nuclear translocation of p65 mainly involves targeting the nuclear localization signal (NLS) of p65, target importins, and blockage of the transactivation domain (TAD) of p65 [46]. Phosphorylation on different residues of p65 induces a conformational change that may facilitate its association with other transcriptional cofactors and affect inflammation [47]. Ser536 is located in the transactivation domain of p65 [48]. Phosphorylation of the Ser536 residue of p65 is an important requisite for negative regulation of the NF-κB signaling pathway but not for the nuclear translocation of p65 [49]. We found that SLC26A4 knockdown suppressed the nuclear translocation of p65 and reduced the phosphorylation of its Ser536 residue, suggesting that SLC26A4 inhibited the NF-κB signaling pathway. However, the detailed mechanism by which the inhibition of SLC26A4 could block the nuclear translocation of p65 has not been elucidated in this study. Herein, the inhibition of SLC26A4 reduced the expression of pro-inflammatory genes, similar to the results that SLC26A4 knockdown inhibited the phosphorylation of Ser536 residue of p65 protein and suggests the mechanism that this phosphorylation in p65 TAD negatively regulates the NF-κB signaling pathway. Hence, the NF-κB signaling pathway might be a mediator of SLC26A-promoted inflammatory responses. In the introduction section of this study, we highlighted a positive correlation of SLC26A4 with inflammatory cytokine levels in various diseases; the current study verifies this correlation.

In conclusion, we found that SLC26A4 promotes myocardial IR injury. Particularly, the most intriguing finding is the potential regulatory relationship between SLC26A4 and the NF-κB signaling pathway and inflammation. In addition, the up-regulation of SLC26A4 by EA pretreatment revealed a potentially important role of SLC26A4 in the alleviation of myocardial IR injury. At last, this study contributes to the current understanding of the effects of SLC26A4 on myocardial IR injury.

Acknowledgement: We would like to express gratitude to the support of the Fourth Affiliated Hospital of Heilongjiang University of Chinese Medicine.

Funding Statement: This study was funded by the Joint Guidance Project of Heilongjiang Provincial Natural Science Foundation of China (LH2023H063) and the Scientific Research Project of Academic Thought Inheritance of Chinese Medicine Great Master of Heilongjiang Provincial Administration of Traditional Chinese Medicine (ZHY2023-151).

Author Contributions: F Kong and Y Kong conceived and supervised the project. F Kong, QY Tian, and BL Kuang designed and performed the experiments. LL Shang, XX Zhang, and DY Li performed the bioinformatics analyses of RNA-seq data. All authors contributed to the writing of the manuscript, reviewed the results, and approved the final version of the manuscript.

Availability of Data and Materials: The datasets generated during and/or analysed during the current study are available from the corresponding author on reasonable request.

Ethics Approval: All animal experiments were approved by the Ethics Committee of the Fourth Affiliated Hospital of Heilongjiang University of Chinese Medicine (No. 19 in 2022). The animal experiments were performed in accordance with the ARRIVE guidelines.

Conflicts of Interest: The authors declare that they have no conflicts of interest to report regarding the present study.

Supplementary Materials: The supplementary material is available online at http://doi.org/10.32604/biocell.2024.046342.

References

1. Boateng S, Sanborn T. Acute myocardial infarction. Dis Mon. 2013;59(3):83–96.
2. Thom T, Haase N, Rosamond W, Howard VJ, Rumsfeld J, Manolio T, et al. Heart disease and stroke statistics—2006 update: a report from the American heart association statistics committee and stroke statistics subcommittee. Circulation. 2006;113(6):e85–151.
3. Lu M, Jia M, Wang Q, Guo Y, Li C, Ren B, et al. The electrogenic sodium bicarbonate cotransporter and its roles in the myocardial ischemia-reperfusion induced cardiac diseases. Life Sci. 2021; 270:119153.
4. Hausenloy DJ, Yellon DM. Myocardial ischemia-reperfusion injury: a neglected therapeutic target. J Clin Invest. 2013; 123(1):92–100.
5. Eltzschig HK, Eckle T. Ischemia and reperfusion—from mechanism to translation. Nat Med. 2011;17(11):1391–401.
6. Wei Z, Qiao S, Zhao J, Liu Y, Li Q, Wei Z, et al. miRNA-181a over-expression in mesenchymal stem cell-derived exosomes influenced inflammatory response after myocardial ischemia-reperfusion injury. Life Sci. 2019;232:116632.
7. Lu S, Tian Y, Luo Y, Xu X, Ge W, Sun G, et al. Iminostilbene, a novel small-molecule modulator of PKM2, suppresses macrophage inflammation in myocardial ischemia-reperfusion injury. J Adv Res. 2021;29:83–94.
8. Makhlouf AM, Chitikova Z, Pusztaszeri M, Berczy M, Delucinge-Vivier C, Triponez F, et al. Identification of CHEK1, SLC26A4, c-KIT, TPO and TG as new biomarkers for human follicular thyroid carcinoma. Oncotarget. 2016;7(29):45776–88.
9. Ito T, Li X, Kurima K, Choi BY, Wangemann P, Griffith AJ. *Slc26a4*-insufficiency causes fluctuating hearing loss and stria vascularis dysfunction. Neurobiol Dis. 2014;66:53–65.
10. Lee JU, Lee HJ, Kim JN, Kim MK, Kim SR, Chang HS, et al. Effects of ammonium chloride on ozone-induced airway inflammation: the role of Slc26a4 in the lungs of mice. J Korean Med Sci. 2020;35(32):e272.
11. Wall SM. The renal physiology of pendrin (SLC26A4) and its role in hypertension. Novartis Found Symp. 2006;273:231–9.

12. Tang L, Yu X, Zheng Y, Zhou N. Inhibiting SLC26A4 reverses cardiac hypertrophy in H9C2 cells and in rats. PeerJ. 2020;8: e8253.
13. Meischl C, Buermans HP, Hazes T, Zuidwijk MJ, Musters RJ, Boer C, et al. H9c2 cardiomyoblasts produce thyroid hormone. Am J Physiol Cell Physiol. 2008;294(5):C1227–33.
14. Do DC, Zhang Y, Tu W, Hu X, Xiao X, Chen J, et al. Type II alveolar epithelial cell-specific loss of RhoA exacerbates allergic airway inflammation through SLC26A4. JCI Insight. 2021; 6(14):e148147.
15. Lee EH, Shin MH, Gi M, Park J, Song D, Hyun YM, et al. Inhibition of pendrin by a small molecule reduces lipopolysaccharide-induced acute lung injury. Theranostics. 2020;10(22):9913–22.
16. Lu SF, Wang JM, Yuan J, Yang WX, Chen LY, Zhang T, et al. Electroacupuncture improves cardiac function and reduces infarct size by modulating cardiac autonomic remodeling in a mouse model of myocardial ischemia. Acupunct Med. 2021; 39(6):681–90.
17. Yang L, Yang J, Wang Q, Chen M, Lu Z, Chen S, et al. Cardioprotective effects of electroacupuncture pretreatment on patients undergoing heart valve replacement surgery: a randomized controlled trial. Ann Thorac Surg. 2010;89(3):781–6.
18. Wang Q, Liang D, Wang F, Li W, Han Y, Zhang W, et al. Efficacy of electroacupuncture pretreatment for myocardial injury in patients undergoing percutaneous coronary intervention: a randomized clinical trial with a 2-year follow-up. Int J Cardiol. 2015;194:28–35.
19. Wang N, Ma J, Ma Y, Lu L, Ma C, Qin P, et al. Electroacupuncture pretreatment mitigates myocardial ischemia/reperfusion injury via XBP1/GRP78/Akt pathway. Front Cardiovasc Med. 2021;8:629547.
20. Xiao Y, Chen W, Zhong Z, Ding L, Bai H, Chen H, et al. Electroacupuncture preconditioning attenuates myocardial ischemia-reperfusion injury by inhibiting mitophagy mediated by the mTORC1-ULK1-FUNDC1 pathway. Biomed Pharmacother. 2020;127:110148.
21. Nennig SE, Schank JR. The role of NFkB in drug addiction: beyond inflammation. Alcohol Alcohol. 2017;52(2):172–9.
22. Lawrence T. The nuclear factor NF-κB pathway in inflammation. Cold Spring Harb Perspect Biol. 2009;1(6):a001651.
23. Dong P, Liu K, Han H. The role of NF-κB in myocardial ischemia/reperfusion injury. Curr Protein Pept Sci. 2022;23(8): 535–47.
24. Yao Y, Li F, Zhang M, Jin L, Xie P, Liu D, et al. Targeting CaMKII-δ9 ameliorates cardiac ischemia/reperfusion injury by inhibiting myocardial inflammation. Circ Res. 2022;130(6): 887–903.
25. Ye Y, Birnbaum Y, Widen SG, Zhang Z, Zhu S, Bajaj M, et al. Acupuncture reduces hypertrophy and cardiac fibrosis, and improves heart function in mice with diabetic cardiomyopathy. Cardiovasc Drugs Ther. 2020;34(6):835–48.
26. Park JY, Namgung U. Electroacupuncture therapy in inflammation regulation: current perspectives. J Inflamm Res. 2018;11:227–37.
27. Wang ZG, Liu ZF, Gao Y, Chen YX, Yin CP, Wang QJ. Effects of electroacupuncture pretreatment on long-term postoperative cognitive dysfunction and neuron-inflammation in aged rats. Zhen Ci Yan Jiu. 2023;48(6):557–63.
28. Mai W, Fan YS, Miao FR, He C, Huang LL, Zhao XJ, et al. Effect of electroacupuncture combined with Zhuang-medicine-thread moxibustion on silent information regulator-1/nuclear factor κB signaling pathway in gastric antrum of diabetic gastroparesis rats. Zhen Ci Yan Jiu. 2021;46(10):837–44 (In Chinese).
29. Cao Q, Liu J, Chen S, Han Z. Effects of electroacupuncture at neiguan on myocardial microcirculation in rabbits with acute myocardial ischemia. J Tradit Chin Med. 1998;18(2):134–9.
30. Tsou MT, Huang CH, Chiu JH. Electroacupuncture on PC6 (Neiguan) attenuates ischemia/reperfusion injury in rat hearts. Am J Chin Med. 2004;32(6):951–65.
31. Guo HH, Jing XY, Chen H, Xu HX, Zhu BM. STAT3 but not STAT5 contributes to the protective effect of electroacupuncture against myocardial ischemia/reperfusion injury in mice. Front Med. 2021;8:649654.
32. Chiu JH, Kuo YL, Lui WY, Wu CW, Hong CY. Somatic electrical nerve stimulation regulates the motility of sphincter of Oddi in rabbits and cats: evidence for a somatovisceral reflex mediated by cholecystokinin. Dig Dis Sci. 1999;44(9):1759–67.
33. Lu SF, Huang Y, Wang N, Shen WX, Fu SP, Li Q, et al. Cardioprotective effect of electroacupuncture pretreatment on myocardial ischemia/reperfusion injury via antiapoptotic signaling. Evid Based Complement Alternat Med. 2016;2016: 4609784.
34. Huang Y, Lu SF, Hu CJ, Fu SP, Shen WX, Liu WX, et al. Electroacupuncture at Neiguan pretreatment alters genome-wide gene expressions and protects rat myocardium against ischemia-reperfusion. Molecules. 2014;19(10):16158–78.
35. Kim BG, Yoo TH, Yoo JE, Seo YJ, Jung J, Choi JY. Resistance to hypertension and high Cl^- excretion in humans with *SLC26A4* mutations. Clin Genet. 2017;91(3):448–52.
36. Fu SP, He SY, Xu B, Hu CJ, Lu SF, Shen WX, et al. Acupuncture promotes angiogenesis after myocardial ischemia through H3K9 acetylation regulation at VEGF gene. PLoS One. 2014;9(4): e94604.
37. Gao J, Zhao Y, Wang Y, Xin J, Cui J, Ma S, et al. Anti-arrhythmic effect of acupuncture pretreatment in the rats subjected to simulative global ischemia and reperfusion—involvement of intracellular Ca^{2+} and connexin 43. BMC Complement Altern Med. 2015;15:5.
38. Bastos AU, Oler G, Nozima BH, Moyses RA, Cerutti JM. BRAF V600E and decreased NIS and TPO expression are associated with aggressiveness of a subgroup of papillary thyroid microcarcinoma. Eur J Endocrinol. 2015;173(4):525–40.
39. Li CY, Liang GY, Yao WZ, Sui J, Shen X, Zhang YQ, et al. Integrated analysis of long non-coding RNA competing interactions reveals the potential role in progression of human gastric cancer. Int J Oncol. 2016;48(5):1965–76.
40. Oeckinghaus A, Ghosh S. The NF-κB family of transcription factors and its regulation. Cold Spring Harb Perspect Biol. 2009; 1(4):a000034.
41. Christian F, Smith EL, Carmody RJ. The regulation of NF-κB subunits by phosphorylation. Cells. 2016;5(1):12.
42. Kashyap T, Argueta C, Aboukameel A, Unger TJ, Klebanov B, Mohammad RM, et al. Selinexor, a selective inhibitor of nuclear export (SINE) compound, acts through NF-κB deactivation and combines with proteasome inhibitors to synergistically induce tumor cell death. Oncotarget. 2016; 7(48):78883–95.
43. Urata M, Kokabu S, Matsubara T, Sugiyama G, Nakatomi C, Takeuchi H, et al. A peptide that blocks the interaction of NF-κB p65 subunit with Smad4 enhances BMP2-induced osteogenesis. J Cell Physiol. 2018;233(9):7356–66.

44. Sundahl N, Bridelance J, Libert C, De Bosscher K, Beck IM. Selective glucocorticoid receptor modulation: new directions with non-steroidal scaffolds. Pharmacol Ther. 2015;152:28–41.
45. Chen D, Zeng S, Huang M, Xu H, Liang L, Yang X. Role of protein arginine methyltransferase 5 in inflammation and migration of fibroblast-like synoviocytes in rheumatoid arthritis. J Cell Mol Med. 2017;21(4):781–90.
46. Giridharan S, Srinivasan M. Mechanisms of NF-κB p65 and strategies for therapeutic manipulation. J Inflamm Res. 2018;11:407–19.
47. Gao J, Xu D. Correlation between posttranslational modification and intrinsic disorder in protein. Pac Symp Biocomput. 2012; 2012:94–103.
48. Fei X, He Y, Chen J, Man W, Chen C, Sun K, et al. The role of toll-like receptor 4 in apoptosis of brain tissue after induction of intracerebral hemorrhage. J Neuroinflammation. 2019;16(1): 234.
49. Pradere JP, Hernandez C, Koppe C, Friedman RA, Luedde T, Schwabe RF. Negative regulation of NF-κB p65 activity by serine 536 phosphorylation. Sci Signal. 2016;9(442):ra85.